Electrochimica Acta 389 (2021) 138748

Contents lists available at ScienceDirect

Electrochimica Acta

journal homepage: www.elsevier.com/locate/electacta

# Electrochemically driven synthesis of phosphorothioates from trialkyl phosphites and aryl thiols

Lingmin Zhao, Xin Liu, Shuxian Shi, Zengzhi Wu, Xiaqun Guo, Zhenlu Shen*, Meichao Li*

*College of Chemical Engineering, Zhejiang University of Technology, Hangzhou 310032, China*

ARTICLE INFO

*Article history:*
Received 7 May 2021
Revised 2 June 2021
Accepted 3 June 2021
Available online 8 June 2021

*Keywords:*
Electrochemical oxidation
Trialkyl phosphites
Aryl thiols
Phosphorothioates
KI

ABSTRACT

A facile and elegant protocol for synthesis of phosphorothioates from trialkyl phosphites and aryl thiols via indirect electrochemical oxidation mediated by KI has been successfully developed. KI as a redox mediator, enabled the reaction of trialkyl phosphites and aryl thiols effectively at low potential. Cyclic voltammetry and *in situ* FTIR were applied to investigate the electrocatalytic activity of KI for the cross-coupling of trialkyl phosphites with aryl thiols. A variety of phosphorothioates were obtained in good to excellent yields under the optimal conditions. This strategy provided an expedient access to construct P–S bond with good functional group compatibility and a broad substrate scope.



## 1. Introduction

Phosphorothioates with P–S bond motifs have a wide range of application in agricultural chemistry, organic synthesis and medicinal chemistry [1–3]. Most of them possess notable bioactivities, such as suppression of HIV expression [4], inhibition of cholinesterases [5], and inhibitory activity to AChE [6]. In light of the significance of phosphorothioates, numerous methodologies have been explored to prepare them. Timperley's team described an approach to synthesize phosphorothioates through cross-coupling reactions of thiols with phosphorochloridates or phosphorobromidates [7]. Nevertheless, it was necessary to prepare the reactants phosphorochloridates or phosphorobromidates before the synthesis, which often involved the toxic halogen such as chlorine or bromine. Recently, cross-coupling reactions of H-phosphonates with thiols have been reported using transition-metals, such as Pd [8], Fe [9], Cu [10] and Ni [11]. An efficient approach for synthesis of phosphorothioates via Pd-catalyzed dehydrogenative coupling of H-phosphonates with thiols has been realized in high yields, but the reactions were carried out at about 100 °C for 20 h [8]. A Fe(Pc)-catalyzed oxidative coupling reaction of H-phosphonates and thiols was achieved in the presence of base for 24 h [9]. It could effectively improve the selectivity and yield for the synthesis reactions, but the use of transition-metal catalysts would result in metal residue [12].

With the development of modern organic synthesis chemistry, oxidative cross-coupling reactions without transition metals become more desirable to synthesize phosphorothioates [13–18]. P–S formation reaction to obtain phosphorothioates was performed with 2.0 equiv. di-*tert*-butyl peroxide (DTBP) as the oxidant from H-phosphonates with thiophenols/disulfides at 80 °C for 20 h [14]. Such coupling reaction would also be realized with the oxidant 1,3-dichloro-5,5-dimethylhydantotin in excellent yields [15]. Great progress has been made in this field, but most of these methods should be associated with stoichiometric oxidants.

Over the past decade, electrochemical anodic oxidation provided a mild tool for various organic transformations, which was a green and sustainable synthesis method [19–22]. Instead of the traditional methods, P–Se [23], P–O [24,25], P–C [26–28], P–S [29–31] bonds were successfully constructed by electrochemical oxidation. Zheng et al disclosed a direct electrochemical dehydrogenative cross-coupling of H-phosphine oxide with thiols to construct P–S bond, and put forward a mechanism of free radical pathway [30]. Lee's team reported a method for preparing phosphorothioates from thiols and H-phosphonates through electrochemical reaction, which was carried out under argon atmosphere for 7 h [31]. Their work was very interesting and valuable.

Very recently we reported a simple and convenient method for synthesis of phosphorothioates by the reaction of trialkyl phosphites and thiols with trichloroisocyanuric acid as the oxidant [32]. Inspired by the aforementioned works, and continuation of our work on mercaptan chemistry [33–35], we attempted to build P–S bond to obtain phosphorothioates from trialkyl phosphites and aryl thiols via electrochemical method. The redox properties of reaction

* Corresponding authors.
*E-mail addresses:* zhenlushen@zjut.edu.cn (Z. Shen), limc@zjut.edu.cn (M. Li).

https://doi.org/10.1016/j.electacta.2021.138748
0013-4686/

were investigated by cyclic voltammetry, in suit FTIR, control experiment and electrosynthsis. In addition, a plausible mechanism was proposed on the basis of all the experiments.

## 2. Experimental section

### 2.1. General information

The solvent and other chemical materials were acquired from commercial suppliers and used directly without further purification. Gas chromatography (GC) analysis was recorded at Agilent GC6890 system equipped with a SH-Rtx-Was capillary column and a flame ionization detector (FID). GC-MS analysis was performed on Thermo Trace ISQ instrument with TG 5 MS capillary column. $^{13}C$ NMR and $^{1}H$ NMR spectra for 125 MHz and 500 MHz were measured on a Bruker Avance III spectrometer. Tetramethylsilane was used as the interal standard and $CDCl_3$ as the solvent.

### 2.2. Electrochemical characterization

Cyclic voltammetry measurements were carried out on CHI600e electrochemical workstation (CH Instrument Inc. Austin, TX, USA). The experiments were measured with an L-type Pt electrode (3 mm diameter) as the working electrode in a 25 mL undivided cell with acetonitrile ($CH_3CN$) as the solvent and sodium tetrafluoroborate ($NaBF_4$) as the supporting electrolyte. Another Pt electrode (1.5 cm × 1.5 cm) was employed as the counter electrode and $Ag/Ag^+$ electrode (0.1 mol/L $AgNO_3$ in $CH_3CN$) was as the reference electrode.

*In situ* FTIR spectroscopy experiments were measured on Nicolet 670 FTIR spectrometer, which was equipped with liquid-nitrogen-cooled MCT-A detector. The working electrode was a Pt disk (6 mm in diameter). A three-electrode spectro-electrochemical cell with $CaF_2$ window at the bottom was used. The reference potential was selected at -600 mV. Each spectrum was collected at 8 $cm^{-1}$ resolution at different potential.

### 2.3. Typical electrolysis experiments

Electrolysis experiments were performed in a 25 mL undivided cell using Vertex Potentiostat/Galvanostat. Two Pt electrodes (1.5 cm × 1.5 cm) were employed as the working electrode and the counter electrode, respectively. The $Ag/Ag^+$ electrode (0.1 mol/L $AgNO_3$ in $CH_3CN$) was used as the reference electrode. $NaBF_4/CH_3CN$ solution (0.1 mol/L, 15 mL), triethyl phosphite (**1a**, 0.5 mmol), 4-methylbenzenethiol (**2a**, 0.9 mmol) and KI (0.08 mmol) were added into the cell. Then the electrolysis reaction was carried out at the potential of 0.2 V at 40 °C with stirring. When the reaction was finished (monitored by GC or TLC), the resulting mixture was concentrated under reduced pressure. Finally, the residue was purified by column chromatography on silica gel using petroleum ether : ethyl acetate (8 : 1) as eluent to afford *O,O*-diethyl *S*-(*p*-tolyl) phosphorothioate (**3aa**) as colorless oil in 85% yield.

### 2.4. Characterization data of products

#### 2.4.1. O,O-Diethyl S-(p-tolyl) phosphorothioate (*3aa*)

Colorless oil (110.5 mg, 0.43 mmol, 85% yield). $^{1}H$ NMR (500 MHz, $CDCl_3$) $\delta$ 7.46-7.44 (m, 2H), 7.15 (d, $J$ = 8.0 Hz, 2H), 4.24-4.13 (m, 4H), 2.35 (d, $J$ = 1.8 Hz, 3H), 1.33-1.30 (m, 6H); $^{13}C$ NMR (125 MHz, $CDCl_3$) $\delta$ 139.2 (d, $J$ = 3.8 Hz), 134.5 (d, $J$ = 5 Hz), 130.1 (d, $J$ = 2.5 Hz), 122.8 (d, $J$ = 7.5 Hz), 63.91 (d, $J$ = 6.3 Hz), 21.1, 15.9 (d, $J$ = 5 Hz). MS(EI), m/z 260.11 [M+, 35%], 124.02 (100%).

#### 2.4.2. O,O-Diethyl S-(o-tolyl) phosphorothioate (*3ab*)

Colorless oil (104.9 mg, 0.40 mmol, 81% yield). $^{1}H$ NMR (500 MHz, $CDCl_3$) $\delta$ 7.62-7.61 (m, 1H), 7.28-7.27 (m, 2H), 7.20-7.16 (m, 1H), 4.21-4.11 (m, 4H), 2.53 (d, $J$ = 1.2 Hz, 3H), 1.31-1.28 (m, 6H); $^{13}C$ NMR (125 MHz, $CDCl_3$) $\delta$ 141.9 (d, $J$ = 5.0 Hz), 135.8 (d, $J$ = 3.8 Hz), 130.5 (d, $J$ = 2.5 Hz), 129.0 (d, $J$ = 2.5 Hz), 126.4 (d, $J$ = 3.8 Hz), 125.4 (d, $J$ = 7.5 Hz), 63.8 (d, $J$ = 7.5 Hz), 21.0, 15.7 (d, $J$ = 6.3 Hz). MS(EI), m/z 260.13 [$M^+$, 41%], 91.18 (100%).

#### 2.4.3. O,O-Diethyl S-(m-tolyl) phosphorothioate (3*ac*)

Colorless oil (107.5 mg, 0.41 mmol, 83% yield). $^{1}H$ NMR (500 MHz, $CDCl_3$) $\delta$ 7.38 (d, $J$ = 12.1 Hz, 2H), 7.28-7.23 (m, 1H), 7.17 (d, $J$ = 7.6 Hz, 1H), 4.27-4.14 (m, 4H), 2.36 (s, 3H), 1.34-1.26 (m, 6H); $^{13}C$ NMR (125 MHz, $CDCl_3$) $\delta$ 139.2, 135.2 (d, $J$ = 5.0 Hz), 131.6 (d, $J$ = 5.0 Hz), 129.9, 129.1 (d, $J$ = 2.5 Hz), 126.2 (d, J = 8.8 Hz), 64.0 (d, $J$ = 6.3 Hz), 21.3, 16.0 (d, $J$ = 7.5 Hz). MS(EI), m/z 259.99 [$M^+$, 35%], 124.13 (100%).

#### 2.4.4. O,O-Diethyl S-(4-methoxyphenyl) phosphorothioate (3*ad*)

Colorless oil (114.7 mg, 0.46 mmol, 83% yield). $^{1}H$ NMR (500 MHz, $CDCl_3$) $\delta$ 7.48-7.46 (m, 2H), 6.89 (d, $J$ = 8.7 Hz, 2H), 4.23-4.12 (m, 4H), 3.81 (s, 3H), 1.33-1.30 (m, 6H). $^{13}C$ NMR (125 MHz, $CDCl_3$) $\delta$ 160.5 (d, $J$ = 2.5 Hz), 136.3 (d, $J$ = 5.0 Hz), 116.6 (d, $J$ = 7.5 Hz), 115.0 (d, $J$ = 1.3 Hz), 64.0 (d, $J$ = 6.3 Hz), 55.3, 16.0 (d, $J$=7.5 Hz). MS(EI), m/z 276.05 [$M^+$, 62%], 139.95 (100%).

#### 2.4.5. O,O-Diethyl S-(4-isopropylphenyl) phosphorothioate (*3ae*)

Colorless oil (125.3 mg, 0.44 mmol, 87% yield).$^{1}H$ NMR (500 MHz, $CDCl_3$) $\delta$ 7.49-7.47 (m, 2H), 7.21 (d, $J$ = 8.3 Hz, 2H), 4.25-4.15 (m, 4H), 2.93-2.88 (m, 1H), 1.33-1.30 (m, 6H), 1.24 (d, $J$ = 7.0 Hz, 6H); $^{13}C$ NMR (125 MHz, $CDCl_3$) $\delta$ 150.1 (d, $J$ = 3.8 Hz), 134.7 (d, $J$ = 3.8 Hz), 127.6 (d, $J$ = 2.5 Hz), 123.0 (d, $J$ = 6.3 Hz), 64.0, 33.8, 23.8, 16.0 (d, $J$ = 6.3 Hz). MS(EI), m/z 288.05 [$M^+$, 8%], 91.00 (100%).

#### 2.4.6. S-(4-(tert-Butyl)phenyl) O,O-diethyl phosphorothioate (*3af*)

Colorless oil (105.0 mg, 0.36 mmol, 70% yield).$^{1}H$ NMR (500 MHz, $CDCl_3$) $\delta$ 7.50-7.47 (m, 2H), 7.37 (d, $J$ = 8.4 Hz, 2H), 4.25-4.15 (m, 4H), 1.33-1.30 (m, 15H); $^{13}C$ NMR (125 MHz, $CDCl_3$) $\delta$ 152.4 (d, $J$ = 3.8 Hz), 134.3 (d, $J$ = 5.0 Hz), 126.5 (d, $J$ = 1.3 Hz), 122.8 (d, $J$ = 6.3 Hz), 64.0 (d, $J$ = 5.0 Hz), 34.7, 31.2, 16.0 (d, $J$ = 7.5 Hz). MS(EI), m/z 301.81 [$M^+$, 8%], 70.08 (100%).

#### 2.4.7. O,O-Diethyl S-(4-fluorophenyl) phosphorothioate (*3ag*)

Colorless oil (108.6 mg, 0.41 mmol, 82% yield). $^{1}H$ NMR (500 MHz, $CDCl_3$) $\delta$ 7.57-7.54 (m, 2H), 7.07-7.04 (m, 2H), 4.25-4.12 (m, 4H), 1.33-1.30 (m, 6H); $^{13}C$ NMR (125 MHz, $CDCl_3$) $\delta$ 163.4 (dd, $J$ = 249, 2.5 Hz), 136.7 (dd, $J$ = 13.8, 5.0 Hz), 121.7 (dd, $J$ = 11.3, 3.8 Hz), 116.5 (dd, $J$ = 25, 1.3 Hz), 64.2 (d, $J$ = 6.3 Hz), 16.0 (d, $J$ = 6.3 Hz). MS(EI), m/z 263.86 [$M^+$, 10%], 82.93 (100%).

#### 2.4.8. S-(4-Chlorophenyl) O,O-diethyl phosphorothioate (*3ah*)

Colorless oil (126.0 mg, 0.45 mmol, 90% yield). $^{1}H$ NMR (500 MHz, $CDCl_3$) $\delta$ 7.51-7.49 (m, 2H), 7.32 (d, $J$ = 8.5 Hz, 2H), 4.24-4.14 (m, 4H), 1.33-1.25 (m, 6H); $^{13}C$ NMR (125 MHz, $CDCl_3$) $\delta$ 135.8 (d, $J$ = 6.3 Hz), 135.5 (d, $J$ = 2.5 Hz), 129.5 (d, $J$ = 1.3 Hz), 125.1 (d, $J$ = 7.5 Hz), 64.2 (d, $J$ = 6.3 Hz), 16.0 (d, $J$ = 7.5 Hz). m/z 279.90 [$M^+$, 10%], 108.93 (100%).

#### 2.4.9. S-(4-Bromophenyl) O,O-diethyl phosphorothioate (*3ai*)

Colorless oil (138.0 mg, 0.42 mmol, 85% yield). $^{1}H$ NMR (500 MHz, $CDCl_3$) $\delta$ 7.47 (d, $J$ = 8.6 Hz, 2H), 7.44-7.42 (m, 2H), 4.24-4.12 (m, 4H), 1.33-1.30 (m, 6H); $^{13}C$ NMR (125 MHz, $CDCl_3$) $\delta$ 135.9 (d, $J$ = 5.0 Hz), 132.5 (d, $J$ = 2.5 Hz), 125.8 (d, $J$ = 7.5 Hz), 123.6 (d, $J$ = 3.8 Hz), 64.2 (d, $J$ = 6.3 Hz), 16.0 (d, $J$ = 6.3 Hz). MS(EI), m/z 323.80 [$M^+$, 8%], 109.06 (100%).

*2.4.10. S-(2,4-Dimethylphenyl) O,O-diethyl phosphorothioate (**3aj**)*

Colorless oil (104.7 mg, 0.38 mmol, 76% yield). $^1$H NMR (500 MHz, $CDCl_3$) $\delta$ 7.49-7.47 (m, 1H), 7.08 (s, 1H), 7.00-6.98 (m, 1H), 4.23-4.10 (m, 4H), 2.49 (s, 3H), 2.31 (d, $J$ = 2.1 Hz, 3H), 1.32-1.29 (m, 6H); $^{13}$C NMR (125 MHz, $CDCl_3$) $\delta$ 142.1 (d, $J$ = 5.0 Hz), 139.7 (d, $J$ = 3.8 Hz), 136.2 (d, $J$ = 5.0 Hz), 131.7 (d, $J$ = 1.3 Hz), 127.6 (d, $J$ = 2.5 Hz), 122.0 (d, $J$ = 6.3 Hz), 64.0 (d, $J$ = 6.3 Hz), 21.3, 21.1, 16.0 (d, $J$ = 7.5 Hz), MS(EI), m/z 273.97 [$M^+$, 10%], 105.12 (100%).

*2.4.11. O,O-Diethyl S-(naphthalen-2-yl) phosphorothioate (**3ak**)*

Colorless oil (123.8 mg, 0.42 mmol, 84% yield). $^1$H NMR (500 MHz, $CDCl_3$) $\delta$ 8.10 (s, 1H), 7.86-7.80 (m, 3H), 7.63 (d, $J$ = 8.6 Hz, 1H), 7.54-7.51 (m, 2H), 4.29-4.17 (m, 4H), 1.34-1.31 (m, 6H); $^{13}$C NMR (125 MHz, $CDCl_3$) $\delta$ 134.4 (d, $J$ = 6.8 Hz), 133.6 (d, $J$ = 1.3 Hz), 133.0, 130.9 (d, $J$ = 3.8 Hz), 129.0, 127.7 (d, $J$ = 5.0 Hz), 127.0, 126.7, 123.8 (d, $J$ = 7.8 Hz), 64.1 (d, $J$ = 6.3 Hz), 16.0 (d, $J$ = 6.3 Hz). MS(EI), m/z 296.02 [$M^+$, 12%], 115.10 (100%).

*2.4.12. O,O-Diethyl S-(thiophen-2-yl) phosphorothioate (**3al**)*

Colorless oil (94.5 mg, 0.38 mmol, 75% yield). $^1$H NMR (500 MHz, $CDCl_3$) $\delta$ 7.45-7.43 (m, 1H), 7.28-7.24 (m, 1H), 7.05-7.03 (m, 1H), 4.28-4.20 (m, 4H), 1.37-1.34 (m, 6H); $^{13}$C NMR (125 MHz, $CDCl_3$) $\delta$ 136.1 (d, $J$ = 7.5 Hz), 131.0 (d, $J$ = 3.8 Hz), 127.8 (d, $J$ = 2.5 Hz), 123.2 (d, $J$ = 8.8 Hz), 64.4 (d, $J$ = 6.3 Hz), 16.0 (d, $J$ = 7.5 Hz). MS(EI), m/z 251.96 [$M^+$, 31%], 115.9 (100%).

*2.4.13. O,O-Diethyl S-(benzyl) phosphorothioate (**3am**)*

Colorless oil (62.4 mg, 0.24 mmol, 48% yield). $^1$H NMR (500 MHz, $CDCl_3$) $\delta$ 7.39-7.28 (m, 5H), 4.16-4.12 (m, 2H), 4.07-4.02 (m, 4H), 1.32-1.28 (m, 6H); $^{13}$C NMR (125 MHz, $CDCl_3$) $\delta$ 137.5 (d, $J$ = 5.0 Hz), 128.9, 128.7, 127.6, 63.5 (d, $J$ = 5.0 Hz), 29.7 (d, $J$ = 5.0 Hz), 16.0 (d, $J$ = 6.3 Hz), MS(EI), m/z 260.08 [$M^+$, 30%], 91.03 (100%).

*2.4.14. O,O-Disopropyl S-(p-tolyl) phosphorothioate (**3ba**)*

Colorless oil (128.2 mg, 0.45 mmol, 89% yield). $^1$H NMR (500 MHz, $CDCl_3$) $\delta$ 7.48-7.46 (m, 2H), 7.13 (d, $J$ = 7.95 Hz, 2H), 4.79-4.72 (m, 2H), 2.32 (d, $J$ = 1.2 Hz, 3H), 1.32 (d, $J$ = 6.2 Hz, 6H), 1.25 (d, $J$ = 6.2 Hz, 6H); $^{13}$C NMR (125 MHz, $CDCl_3$) $\delta$ 138.8 (d, $J$ = 2.5 Hz), 134.3 (d, $J$ = 6.3 Hz), 129.9 (d, $J$ = 2.5 Hz), 123.5 (d, $J$ = 7.5 Hz), 73.1 (d, $J$ = 6.3 Hz), 23.8 (d, $J$ = 3.8 Hz), 23.5 (d, $J$ = 6.3 Hz), 21.1. MS(EI), m/z 288.09 [$M^+$, 52%], 153.94 (100%).

*2.4.15. O,O-Dibutyl S-(p-tolyl) phosphorothioate (**3ca**)*

Colorless oil (121.4 mg, 0.38 mmol, 77% yield). $^1$H NMR (500 MHz, $CDCl_3$) $\delta$

7.46-7.43 (m, 2H), 7.15 (d, $J$ = 8.0 Hz, 2H), 4.17-4.05 (m, 4H), 2.34 (d, $J$ = 1.8 Hz, 3H), 1.65-1.60 (m, 4H), 1.38-1.34 (m, 4H), 0.92-0.89 (m, 6H); $^{13}$C NMR (125 MHz, $CDCl_3$) $\delta$ 139.2 (d, $J$ = 3.8 Hz), 134.6 (d, $J$ = 5.0 Hz), 130.1 (d, $J$ = 2.5 Hz), 122.9 (d, $J$ = 7.5 Hz), 67.7 (d, $J$ = 7.5 Hz), 32.1 (d, $J$ = 6.3 Hz), 21.1, 18.6, 13.5. MS(EI), m/z 316.04 [$M^+$, 7%], 91.09 (100%).

## 3. Results and discussion

### 3.1. Electrochemical analysis

The electrochemical cross-coupling reaction of triethyl phosphite (**1a**, 0.5 mmol) with 4-methylbenzenethiol (**2a**, 0.9 mmol) catalyzed by KI (0.08 mmol) was carried out in 0.1 mol/L $NaBF_4/CH_3CN$ solution by cyclic voltammetry between -0.6 V and 0.8 V at the scan rate of 50 mV/s. Cyclic voltammogram of KI in $NaBF_4/CH_3CN$ solution was collected and shown in curve b Fig. 1 (A). The specific reaction process of KI on the electrode surface might consist of the following steps [36,37]:

$$3I^- - 2e^- \rightleftharpoons I_3^- \quad (1)$$

$$2I_3^- - 2e^- \rightleftharpoons 3I_2 \quad (2)$$

The oxidation of $I^-$ began at about -0.25 V and the first oxidation peak at -0.07 V might be assigned to the formation of triiodine anion $I_3^-$ (Eq. (1)). The second oxidation peak at 0.32 V might be related to the oxidation of $I_3^-$ to $I_2$ (Eq. (2)). Therefore, $I_3^-$ and $I_2$ were always believed to be the key species in iodine-catalyzed electrochemical reactions and participated in the catalytic cycle to promote the reaction continuously [38–40].

When both of **1a** and KI were added in $NaBF_4/CH_3CN$ solution, the oxidation current for **1a** increased sharply (curve a Fig. 1(A)) by comparison of curve b. In addition, the second peak current related to Eq. (2) disappeared. It was most likely that the oxidation of **1a** was promoted by $I_3^-$. However, without KI under the similiar conditions, almost no voltametric response for the oxidation of **1a** in $NaBF_4/CH_3CN$ solution was observed (curve c). Therefore, **1a** was difficult to be oxidized at low potential directly and its oxidation could be effectively catalyzed by the presence of KI in $NaBF_4/CH_3CN$ solution. Only at high potential, electrochemical oxidation of **1a** could take place in the absence of KI, which could be proved by the cyclic voltammogram shown in curve d Fig 1(B).

Subsequently, the reaction of **2a** and KI has been investigated by cyclic voltammetry. As shown in Fig. 2 (A), there was no obvious oxidation peak when **2a** was added in $NaBF_4/CH_3CN$ solution without KI (curve f), but the oxidation peak current rose sharply with the addition of KI at the potential higher than 0.05 V (curve e). Thus KI played an important role for the oxidation of **2a** [41,42].

*In situ* time-resolved FTIR spectra were applied to analyze the reaction of **2a** and KI in $NaBF_4/CH_3CN$ solution and collected during reaction of **2a** (1.8 mmol) and KI (0.32 mmol) in 0.1 mol/L $NaBF_4/CH_3CN$ solution at the potential of 50 mV. The positive-going and negative-going peaks represent material consumption and product generation respectively [43]. As shown in Fig. 2(B), the positive bands at 2562 and 1495 $cm^{-1}$ were attributed to stretching vibration of S–H band and benzene ring vibration of **2a**, respectively [44]. At the same time, the negative-going peaks at 1485 $cm^{-1}$ represented skeleton vibration of the benzene ring of 1,2-di-*p*-tolyldisulfane which was generated from **2a**. Combined with the results of cyclic voltammetry and *in situ* FTIR, it could be found that 1,2-di-*p*-tolyldisulfane was formed at about 0.05 V.

With the addition of **1a** and **2a** in the $NaBF_4/CH_3CN$ solution in the presence of KI, the current started to rise at about -0.2 V (curve h Fig. 3(A)). Moreover, two oxidation peaks were clearly observed at around 0 V and 0.67 V. The obvious peak at around 0 V might be caused by the reaction of **1a** and **2a** mediated by $I_3^-$. The oxidation peak at about 0.67 V might be related to the reaction of 1,2-di-*p*-tolyldisulfane and **1a**. For comparison, cyclic voltammogram was also collected in $NaBF_4/CH_3CN$ without KI under the similar conditions. It showed that current for electrochemical oxidation of **1a** and **2a** was small at low potential (curve g), illustrating that electro-oxidation reaction of them was quite slow. In order to better understand the electrochemical reaction of **1a** and **2a**, high potential scanning was applied and the result was presented in Fig. 3(B). High anodic current was clearly observed at about 1.90 V (curve i), and it indicated that only high potential helped to realize the high conversion of the reaction without KI.

In addition, the cross-coupling reaction between **1a** and **2a** was also investigated with *in situ* FTIR technique, which was carried out in 0.1 mol/L $NaBF_4/CH_3CN$ solution in the presence of **1a** (2.0 mmol), **2a** (2.0 mmol) and KI (0.32 mmol) at potentials varied from -600 mV to 300 mV. As shown in Fig. 3(C), four important positive bands at 2562, 1495, 1025 and 926 $cm^{-1}$ and three negative bands at 1258, 1062 and 977 $cm^{-1}$ could be observed. Two important positive-going peaks at 2562 and 1495 $cm^{-1}$ associated with **2a** were observed. The positive bands at 1025 and 926 $cm^{-1}$ were

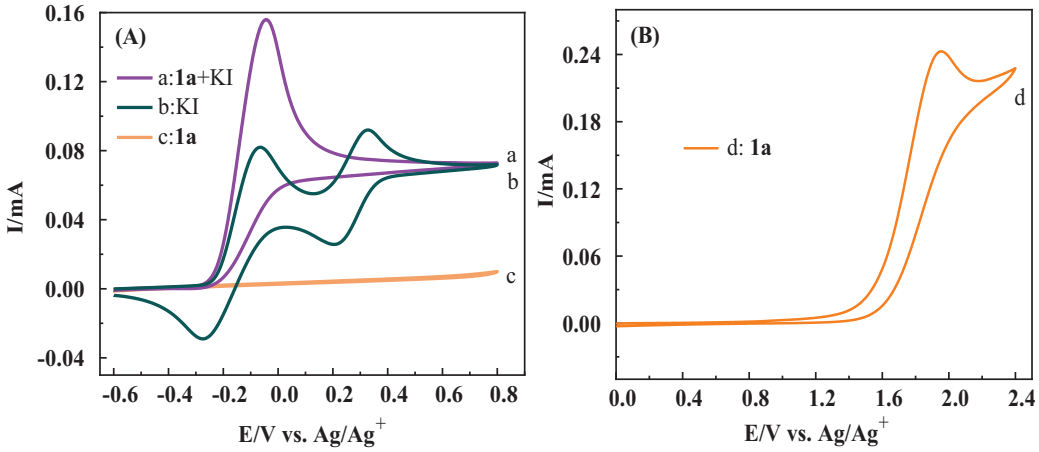


**Fig. 1..** (A) Cyclic voltammograms recorded in 0.1 mol/L $NaBF_4/CH_3CN$ from -0.6 V to 0.8 V at the scan rate of 50 mV/s in the presence of (a) **1a** (0.5 mmol) and KI (0.08 mmol); (b) KI (0.08 mmol); (c) **1a** (0.5 mmol). (B) Cyclic voltammogram recorded in 0.1 mol/L $NaBF_4/CH_3CN$ from 0 V to 2.4 V at the scan rate of 50 mV/s with (d) **1a** (0.5 mmol).

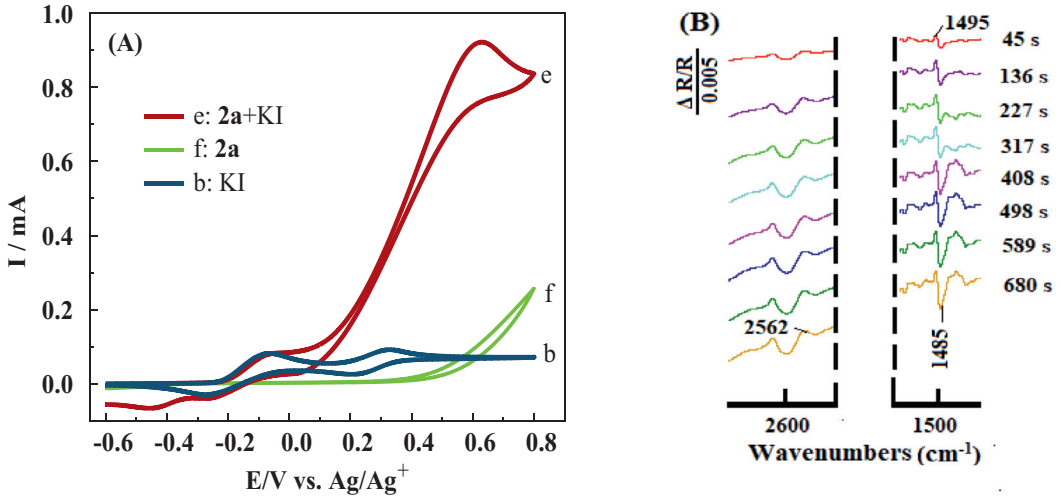


**Fig. 2.** (A) Cyclic voltammograms recorded in 0.1 mol/L $NaBF_4/CH_3CN$ between -0.6 ~ 0.8 V at the scan rate of 50 mV/s in the presence of (b) KI (0.08 mmol); (e) **2a** (0.9 mmol) and KI (0.08 mmol); (f) **2a** (0.9 mmol). (B) *In situ* time-resolved FTIR spectra collected during reaction of **2a** (1.8 mmol) and KI (0.32 mmol) in 0.1 mol/L $NaBF_4/CH_3CN$ solution at the potential of 50 mV.

attributed to stretching vibrations C–O(P) and P–O(C) of **1a**, respectively [45]. The four positive bands were related to the consumption of **1a** and **2a**.

The negative band at 1062 $cm^{-1}$ was attributed to the stretching vibration C–O(P). When the valence of phosphorus changes from 3 to 5, the absorption peak of P–O shifted to a high wave number value [45,46]. Thus the negative peak at 977 $cm^{-1}$ was assigned to the stretching vibration of P–O single bond of **3aa**. In addition, the P=O bond formed at 1258 $cm^{-1}$ was increased with the depletion of **1a** [45,47]. Based on the above infrared analysis, the corresponding product **3aa** has been generated. So synthesis of **3aa** could be carried out sucessfully from **1a** and **2a** at low potential in the present of KI.

### 3.2. Optimization of electrolysis experiment conditions

As an initial attempt, triethyl phosphite (**1a**) and 4-methylbenzenethiol (**2a**) were selected as the model substrates to ensure the optimal conditions and the results were summarized in Table 1. It was found that a good selectivity to **3aa** (84%) was attained when **1a** reacted with 1.8 equiv. of **2a** in the 0.1 mol/L $NaBF_4/CH_3CN$ solution at the potential of 0.4 V with 10 mol% KI in 4 h (Table 1, entry 1). When the amount of **2a** was decreased to 1.6 equiv., the selectivity to **3aa** declined to 76% (Table 1, entry 2), indicating that the ratio of reactants was an important factor for the reaction. Therefore, the following two reactions were carried out. The reaction with equal equivalent of **1a** and **2a** failed to provide satisfactory result (Table 1, entry 3). A 100% conversion of **2a** with 56% selectivity to **3aa** was obtained by treatment of 1.0 equiv. **2a** with 1.6 equiv. of **1a** (Table 1, entry 4). It showed that excess of **2a** was conducive to the reaction, which might be due to two reasons. On the one hand, excessive **2a** was beneficial to inhibit hydrolysis reactions of **1a** and intermediate, which could improve the selectivity to **3aa** [48]. On the other hand, when **1a** was converted into the target product, the released ethyl radical could react with **2a** to generate the by-product ethyl(*p*-tolyl)sulfane which was detected by GC-MS. Thus, 1.8 equiv. of **2a** was used in the following experiments. Decreasing the loading of KI to 8 mol% gave a lower conversion and selectivity (Table 1, entry 5). An improvement for the selectivity to **3aa** (89%) was obtained when the loading of KI was increased to 12 mol% (Table 1, entry 6). These results encouraged us to further screen the loading of KI (Table 1, entries 7 and 8). It was found that 100% converison of **1a** with 92% selectivity to **3aa** was achieved in the presence of 16

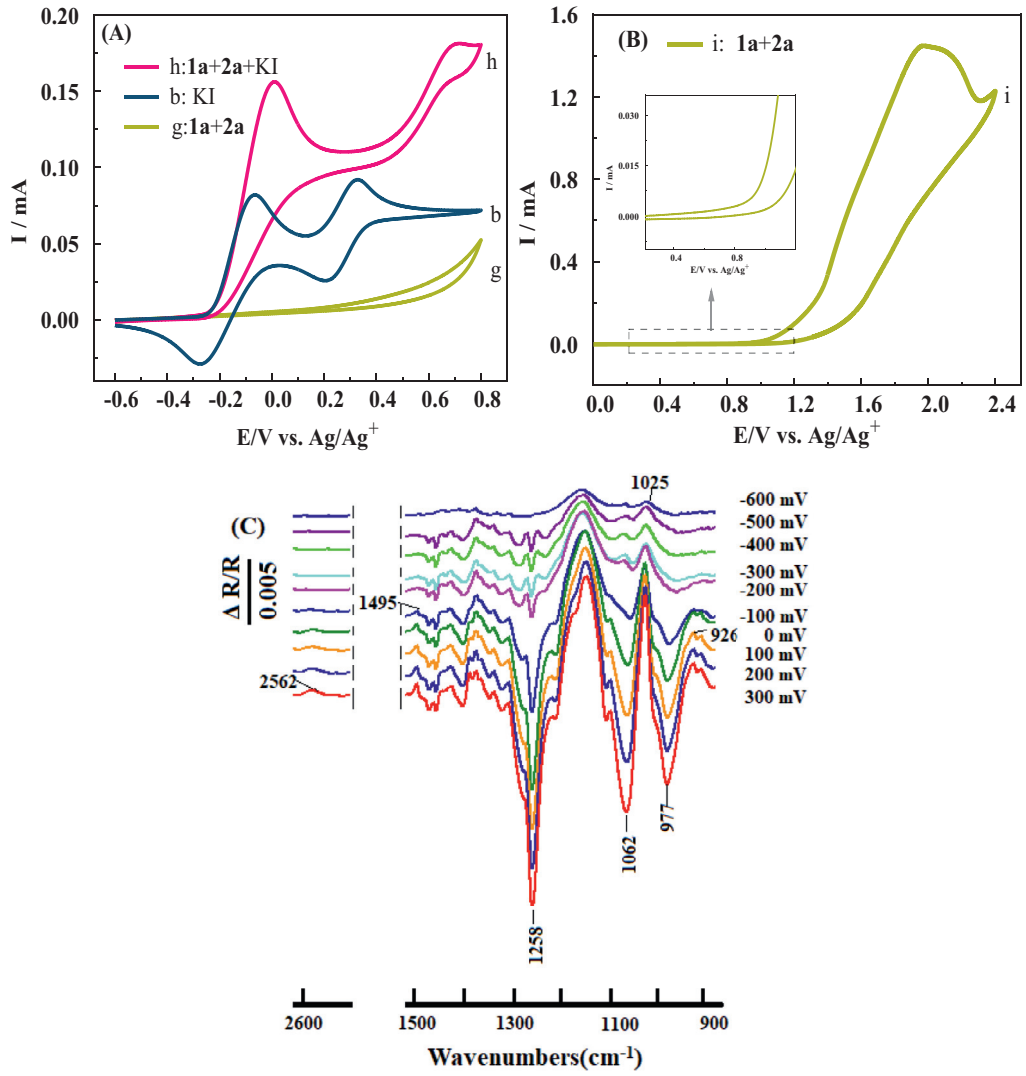


**Fig. 3.** (A) Cyclic voltammograms recorded in 0.1 mol/L $NaBF_4/CH_3CN$ between -0.6 ~ 0.8 V at the scan rate of 50 mV/s in the presence of (g) **1a** (0.5 mmol) and **2a** (0.9 mmol); (b) KI (0.08 mmol); (h) **1a** (0.5 mmol), **2a** (0.9 mmol) and KI (0.08 mmol). (B) Cyclic voltammogram recorded in 0.1 mol/L $NaBF_4/CH_3CN$ between 0 ~ 2.4 V at the scan rate of 50 mV/s in the presence of (i) **1a** (0.5 mmol) and **2a** (0.9 mmol). (C) *In situ* FTIR spectra collected during the reaction of **1a** (2.0 mmol), **2a** (2.0 mmol) and KI (0.32 mmol) in 0.1 mol/L $NaBF_4/CH_3CN$ solution at potentials varied from -600 mV to 300 mV.

mol% of KI. Thus 16 mol% of KI was appropriate for the following experiments. As a comparison, we carried out the reaction under $N_2$ atmosphere, and the result was the same as that under air atmosphere (Table 1, entry 9).

Decreasing the reaction temperature from 40 to 25 °C, the conversion of **1a** was 92% even if the reaction time was prolonged to 6 h (Table 1, entry 10). Thus, 40 °C was chosen for the following experiments. Next, the potential was investigated. When the potential was set at 0.2 V, the conversion of **1a** and selectivity to **3aa** were high as that at 0.4 V (Table 1, entry 11). Therefore, 0.2 V might be high enough for this reaction. In addition, an 81% conversion of **1a** with 90% selectivity to **3aa** was achieved by the use of carbon rod as the anode instead of platinum plate (Table 1, entry 12). Platinum as the anode was slightly better for this reaction. When the reaction of **1a** and **2a** was carried out in $^nBu_4NBF_4/CH_3CN$, the conversion of **1a** was 100% and the selectivity to **3aa** was 88% (Table 1, entry 13). Electrolyte might have little effect on this reaction. Taking into the comprehensive consideration, the optimized conditions for this reaction were performed at 0.2 V under air atmosphere with 16 mol% KI for 4 h in $NaBF_4/CH_3CN$ solution using platinum as the anode and cathode.

### 3.3. Control experiments and plausible mechanism

To gain insight into the reaction mechanism, a series of control experiments were conducted (Scheme 1). When the reaction of **1a** and **2a** performed under the standard conditions (**1a** (0.5 mmol), **2a** (0.9 mmol), KI (0.08 mmol), $NaBF_4/CH_3CN$ (0.1 mol/L), 0.2 V, 40 °C, 4 h.), the isolated yield of **3aa** was 85% (Scheme 1, Eq. (3)). However, no expected product was observed without electric current (Scheme 1, Eq. (4)), and only trace amount of **3aa** could be detected in the absence of KI (Scheme 1, Eq. (5)). These results revealed that KI and electricity played important roles in this electrochemical reaction. Treatment of **2a** to the standard conditions, 1,2-di-*p*-tolyldisulfane (**4**) could be obtained in excellent isolated yield (Scheme 1, Eq. (6)). Then, 78% isolated yield of **3aa** could be achieved in the reaction of **4** and **1a** (Scheme 1, Eq. (7)). In addition, when TEMPO (2,2,6,6-tetramethyl-1-piperidinyloxy) was added as the radical scavenger, the isolated yield of **3aa** was decreased sharply to 37% (Scheme 1, Eq. (8)). This result showed that a radical pathway might be involved in this reaction. According to Fig. 2(A), **2a** could hardly be oxidized at the potential of -0.1 V. Decreasing the potential to -0.1 V, 26% isolated yield of **3aa**

**Table 1.**
Optimization of electrolysis experiment conditions[a].

| Entry | **1a** (equiv.) | **2a** (equiv.) | Potential (V) | *T* (°C) | KI (mol%) | Conv.[b,c] | Select.[c,d] |
|---|---|---|---|---|---|---|---|
| 1 | 1 | 1.8 | 0.4 | 40 | 10 | 98 | 84 |
| 2 | 1 | 1.6 | 0.4 | 40 | 10 | 98 | 76 |
| 3 | 1 | 1 | 0.4 | 40 | 10 | 67 | 64 |
| 4 | 1.6 | 1 | 0.4 | 40 | 10 | 100 [e] | 56 |
| 5 | 1 | 1.8 | 0.4 | 40 | 8 | 84 | 82 |
| 6 | 1 | 1.8 | 0.4 | 40 | 12 | 98 | 89 |
| 7 | 1 | 1.8 | 0.4 | 40 | 16 | 100 | 92 |
| 8 | 1 | 1.8 | 0.4 | 40 | 20 | 100 | 93 |
| 9 [f] | 1 | 1.8 | 0.4 | 40 | 16 | 100 | 92 |
| 10 [g] | 1 | 1.8 | 0.4 | 25 | 16 | 92 | 92 |
| **11** | **1** | **1.8** | **0.2** | **40** | **16** | **100** | **92** |
| 12 [h] | 1 | 1.8 | 0.2 | 40 | 16 | 81 | 90 |
| 13 [i] | 1 | 1.8 | 0.2 | 40 | 16 | 100 | 88 |

[a] Electrolytic conditions: **1a** (0.5 mmol), Pt anode, Pt cathode, 0.1 mol/L $NaBF_4/CH_3CN$ solution (15 mL), 4 h.
[b] Conversion of **1a**.
[c] Determined by GC with peak area normalization method.
[d] Selectivity to **3aa**.
[e] Conversion of **2a**.
[f] Under $N_2$ atmosphere.
[g] Reaction time: 6 h.
[h] C anode, Pt cathode.
[i] 0.1 mol/L $^nBu_4NBF_4/CH_3CN$ solution (15 mL).

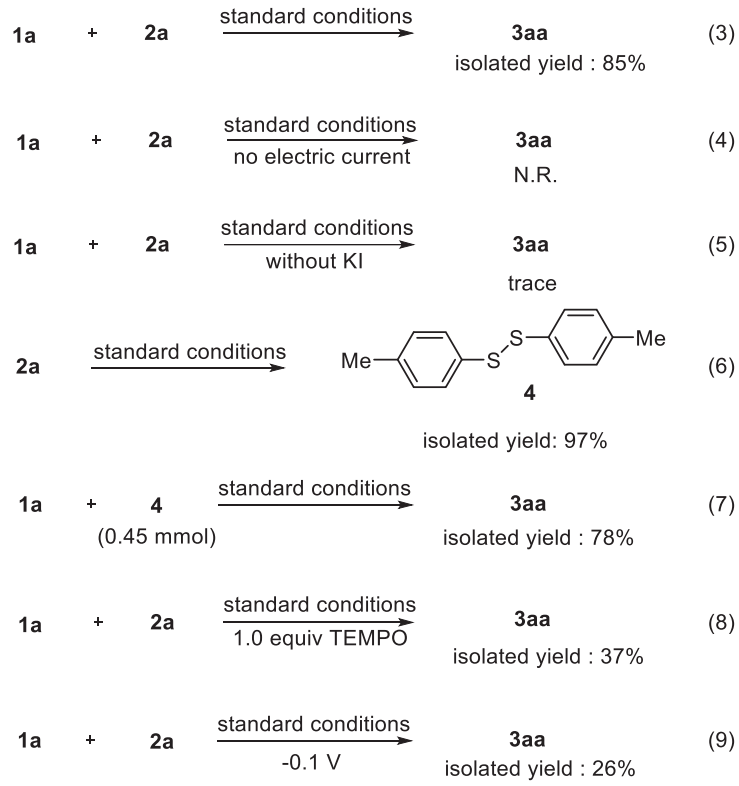


**Scheme 1.** Control experiments. Standard conditions: **1a** (0.5 mmol), **2a** (0.9 mmol), KI (0.08 mmol), $NaBF_4/CH_3CN$ (0.1 mol/L), 0.2 V, 40 °C, 4 h.

was obtained by the reaction of **1a** and **2a** in the presence of KI (Scheme 1, Eq. (9)). It indicated that **2a** could be involved directly in this reaction without previous oxidation.

Based on control experiment results and literatures, a plausible mechanism was proposed in Scheme 2. Initially, $I^-$ was oxidized to $I_3^-$ at the anode, and then iodophosphate **5** was formed from **1a** and $I_3^-$. Iodophosphate **5** would easily react with **2a** by nucleophilic substitution, giving the desired product **3aa** [49,50].

In addition, another pathway might be involved in this reaction. Disulfide **4** was formed from **2a** in the presence of $I_2$. Radical **6** would be generated by homolytically cleavage of disulfide **4** [51,52]. After radical **6** was captured by $P(OEt)_3$, radical intermediate **7** was formed. Then the product **3aa** was produced via $\beta$ scission of ethoxyl group [53–55]. Finally, radical **6** reacted with ethyl radical to produce the side product ethyl(*p*-tolyl)sulfane (**8**) which could be detected in the reaction mixture.

### *3.4. Coupling of aryl thiols with trialkyl phosphites by indirect electro-oxidation*

With the optimized conditions in hand, we applied this electrochemical system for the cross-coupling of aryl thiols with tri-

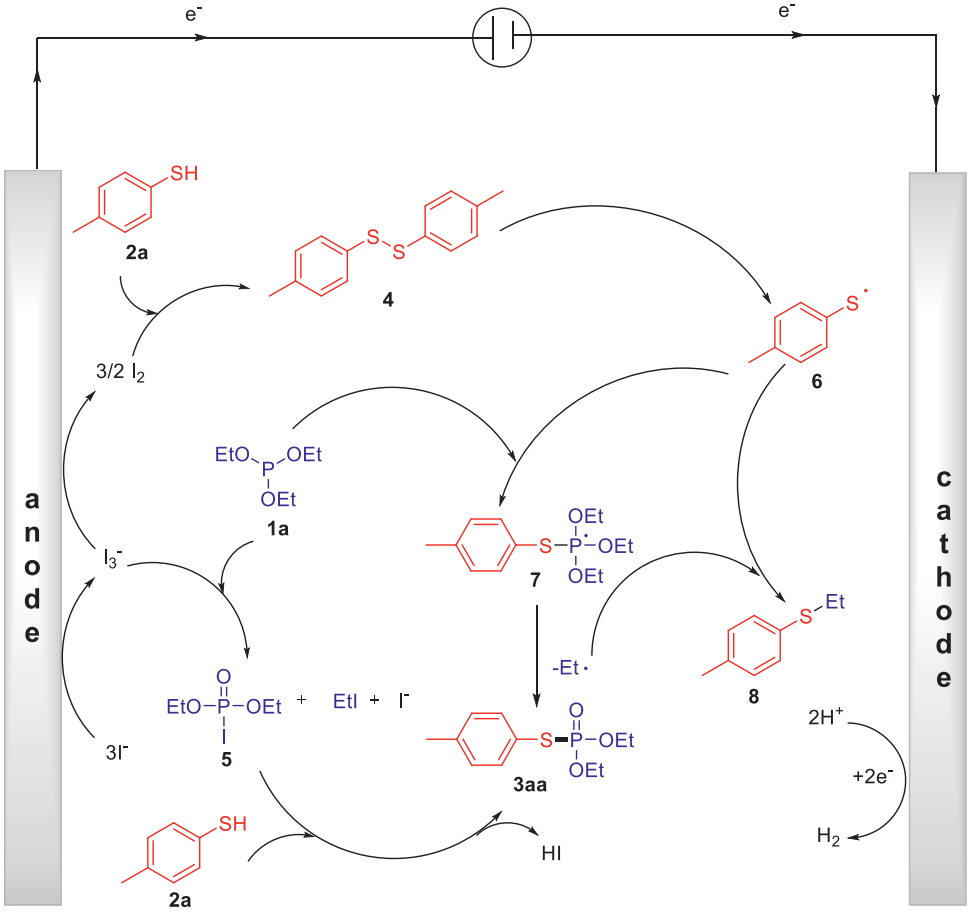


**Scheme 2.** Plausible mechanism.

alkyl phosphites. Firstly, the coupling of triethyl phosphite (**1a**) with a variety of thiophenols (**2a**–**m**) was investigated, and the results were shown in the Table 2. The reactions of *p, o, m*-methylbenzenethiols with **1a** gave the corresponding phosphorothioates **3aa, 3ab** and **3ac** in 85%, 81% and 83% isolated yields respectivily, which could be inferred that steric hindrance had little effect on the reaction. Benzenethiols bearing electron-rich or electron-neutral substituents such as *p*-$OCH_3$, *p*-$^{i}$Pr and *p*-$^{n}$Bu underwent coupling with **1a** smoothly to provide the desired phosphorothioates **3ad–af** in 70%–87% isolated yields. Furthermore, aryl thiols with electron withdrawing groups (*p*-F, *p*-Cl and *p*-Br) could successfully couple with **1a** to afford the corresponding products (**3ag–ai**) in high isolated yields. When 2,4-dimethylbenzenethiol was subjected to the reaction, *S*-(2,4-dimethylphenyl) *O,O*-diethyl phosphorothioate (**3aj**) could be obtained in 76% isolated yield.

In addition to these benzenethiols, naphthalene-2-thiol worked well with **1a** under the standard conditions to gave the product **3ak** in 85% isolated yield. Pleasingly, the scope of the aryl thiols could be extended to heteroaromatic benzenethiol. For example, when thiophene-2-thiol was used as the substrate, the isolated yield of **3al** was 75%. Besides, benzyl mercaptan **(2m)** could react with **1a** to form the desired product in 48% isolated yield. Relevant attempts about aliphatic compounds have also been carried out. It was a pity that only trace amount of target products could be detected. The scope of trialkyl phosphites was also investigated. Both triisopropyl phosphite (**1b**) and tributyl phosphite (**1c**) could react with 4-methylbenzenethiol smoothly, and the desired products **3ba** and **3ca** were achieved in good isolated yields.

### *3.5. Coupling of aryl thiols with trialkyl phosphites by galvanostatic electrolysis*

Potentiostatic electrolysis and galvanostatic electrolysis have their own unique advantages, and have a wide range of applications in electrochemical synthesis. Therefore, galvanostatic electrolysis experiments have also been performed and the results were shown in Table 3. According to Faraday's law, the required electrolysis time were 965 s, 2412 s and 9648 s, respectiviely, when the electrolysis current were 50 mA, 20 mA and 5 mA. However, only 40% conversion of **1a** with 70% selectivity to **3aa** was obtained at 50 mA for 965 s (Table 3, entry 1). Conducting this reaction at 20 mA for 2412 s gave 56% conversion of **1a** and 83% selectivity to **3aa** (Table 3, entry 2). When the reaction was performed at 5 mA for 9648 s, the conversion of **1a** and the selectivity to **3aa** were increased to 69% and 86% respectively (Table 3, entry 3). Prolonging the reaction time to 14400 s, **1a** could be completely converted with 82% selectivity to **3aa** (Table 3, entry 4). These results indicated that more electrolysis time was needed at a low current, but product selectivity was increased.

### *3.6. Coupling of aryl thiols with trialkyl phosphites by direct electrochemical oxidation*

According to Fig. 3(B), the peak current at about 1.90 V for oxidation of **1a** and **2a** in $NaBF_4/CH_3CN$ solution without KI was quite high. Thus, the electrolysis experiments without KI have also been carried out. As shown in Table 4, almost no target product was obtained at the potential of 0.2 V (Table 4, entry 1). Although the selectivity to **3aa** was increased to 56% at the potential of 0.4 V, the

**Table 2**
Electrochemical coupling of trialkyl phosphites with aryl thiols[a].

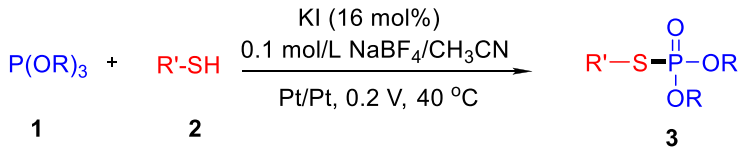


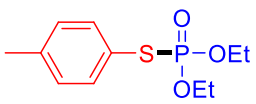
**3aa** 85%

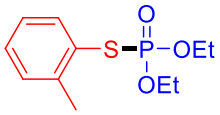
**3ab** 81%

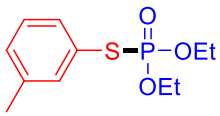
**3ac** 83%

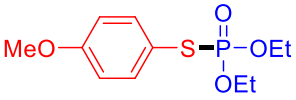
**3ad** 83%

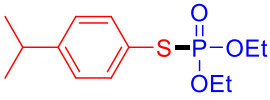
**3ae** 87%

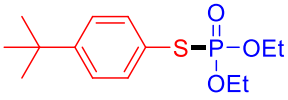
**3af** 70%

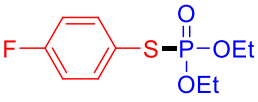
**3ag** 82%

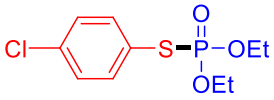
**3ah** 90%

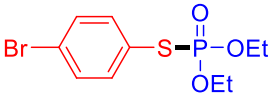
**3ai** 85%

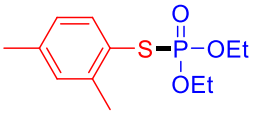
**3aj** 76%

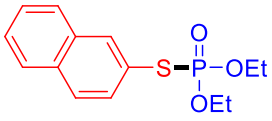
**3ak** 84%

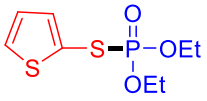
**3al** 75%

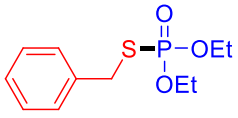
**3am** 48%

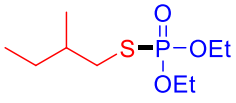
**3an**, trace

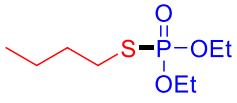
**3ao** trace

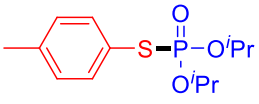
**3ba** 89%

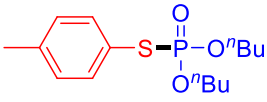
**3ca** 77%

[a] Electrolytic conditions: **1** (0.5 mmol), **2** (0.9 mmol), KI (0.08 mmol), Pt anode, Pt cathode, 0.1 mol/L $NaBF_4/CH_3CN$ solution (15 mL), 0.2 V, 40 °C, 4 h. Isolated yields.

conversion of **1a** was only 17% (Table 4, entry 2). Increasing the potential to 0.9 V, an 89% conversion of **1a** with 30% selectivity to **3aa** was achieved (Table 4, entry 3). Using the potential of 1.4 V gave 98% conversion of **1a** and 17% selectivity to **3aa** (Table 4, entry 4). When the potential was further increased to 1.6 V, the conversion was up to 100%, but the selectivity to **3aa** was decreased to 14% (Table 4, entry 5). A lower selectivity to **3aa** (12%) was obtained at the potential of 1.8 V (Table 4, entry 6). These results indicated that over-oxidation occurred and more by-products would be produced at high potential.

What's more, the reaction of different aryl thiols and **1a** were performed by direct electrochemical oxidation at 0.9 V. It was

**Table 3.**
Galvanostatic electrolysis experiments for **1a** and **2a**[a].

| Entry | Time (s) | Current (mA) | Conv.[b,c] | Select.[c,d] |
|---|---|---|---|---|
| 1 | 965 | 50 | 40 | 70 |
| 2 | 2412 | 20 | 56 | 83 |
| 3 | 9648 | 5 | 69 | 86 |
| 4 | 14400 | 5 | 100 | 82 |

[a] Electrolytic conditions: **1a** (0.5 mmol), **2a** (0,9 mmol), KI (0.08 mmol), Pt anode, Pt cathode, 0.1 mol/L $NaBF_4/CH_3CN$ solution (15 mL), 40 °C
[b] Conversion of **1a**.
[c] Determined by GC with peak area normalization method.
[d] Selectivity to **3aa**.

**Table 4.**
The effect of potential on the direct electrochemical oxidation reaction[a].

| Entry | Potential (V) | Conv.[b,c] | Select.[c,d] |
|---|---|---|---|
| 1 | 0.2 | 10 | <1 |
| 2 | 0.4 | 17 | 56 |
| 3 | 0.9 | 89 | 30 |
| 4 | 1.4 | 98 | 17 |
| 5 | 1.6 | 100 | 14 |
| 6 | 1.8 | 100 | 12 |

[a] Electrolytic conditions: **1a** (0.5 mmol), **2a** (0.9 mmol), Pt anode, Pt cathode, 0.1 mol/L $NaBF_4/CH_3CN$ solution (15 mL), 40 °C, 4 h.
[b] Conversion of **1a**.
[c] Determined by GC with peak area normalization method. [d] Selectivity to **3aa**.

found that aryl thiols with both electron withdrawing (*p*-Cl, *p*-Br) and electron donating groups (*p*-OMe, *p*-$^i$Pr) on the benzene ring gave the desired products in poor GC yields (less than 20%).

## 4. Conclusion

In summary, the cross-coupling of trialkyl phosphites with aryl thiols was achieved by indirect electrochemical oxidation. Only catalytic amount of KI was required in the reaction, and the high reaction efficiency was realized. This reaction provided an oxidant and transition-metal free route with good functional group tolerance. Besides, P–S bond was successfully constructed at a very low potential, which could reduce the side reactions. In addition, cyclic voltammetry and *in situ* FTIR were used to further understand the redox process in the reaction. Combined with a series of control experiments, the possible reaction mechanism was proposed. Meanwhile, the direct electrolysis experiments were performed at high potential and the corresponding products were obtained in low yields, which proved that indirect electrooxidation mediated by KI was more preponderant in this reaction.

## Declaration of Competing Interest

The authors declare that they have no known competing financial interests or personal relationships that could have appeared to influence the work reported in this paper.

## Credit authorship contribution statement

**Lingmin Zhao:** Investigation, Methodology, Writing – original draft. **Xin Liu:** Formal analysis. **Shuxian Shi:** Investigation. **Zengzhi Wu:** Formal analysis. **Xiaqun Guo:** Investigation. **Zhenlu Shen:** Supervision, Writing – review & editing, Funding acquisition. **Meichao Li:** Supervision, Writing – review & editing, Funding acquisition.

## Acknowledgments

This work was financially supported by National Natural Science Foundations of China (21773211 and 21776260) and Key Research and Development Project of Zhejiang Province (No. 2021C01079).

## References

[1] N.S. Li, J.K. Frederiksen, J.A. Piccirilli, Synthesis, properties, and applications of oligonucleotides containing an RNA dinucleotide phosphorothiolate linkage, Acc. Chem. Res. 44 (2011) 1257.
[2] A.M. Lauer, J. Wu, Palladium-catalyzed allylic fluorination of cinnamyl phosphorothioate esters, Org. Lett. 14 (2012) 5138.
[3] T.S. Kumar, T. Yang, S. Mishra, C. Cronin, S. Chakraborty, J.B. Shen, B.T. Liang, K.A. Jacobson, 5'-Phosphate and 5'-phosphonate ester derivatives of (*N*)-methanocarba adenosine with *in vivo* cardioprotective activity, J. Med. Chem. 56 (2013) 902.
[4] T. Kalebic, P.S. Schein, Organic thiophosphate WR-151327 suppresses expression of HIV in chronically infected cells, Aids Res. Hum. Retrovir. 10 (1994) 727.
[5] B. Kaboudin, S. Emadi, A. Hadizadeh, Synthesis of novel phosphorothioates and phosphorodithioates and their differential inhibition of cholinesterases, Bioorg. Chem. 37 (2009) 101.
[6] R.L. Xie, Q.F. Zhao, T. Zhang, J. Fang, X.D. Mei, J. Ning, Y. Tang, Design, synthesis and biological evaluation of organophosphorous-homodimers as dual binding site acetylcholinesterase inhibitors, Bioorg. Med. Chem. 21 (2013) 278.
[7] C.M. Timperley, S.A. Saunders, J. Szpalek, M.J. Waters, Fluorinated phosphorus compounds Part 8. The reactions of bis(fluoroalkyl) phosphorochloridates with sulfur nucleophiles, J. Fluor. Chem. 119 (2003) 161.
[8] Y.Y. Zhu, T.Q. Chen, S. Li, S. Shimada, L.B. Han, Efficient Pd-catalyzed dehydrogenative coupling of P(O)H with RSH: a precise construction of P(O)-S bonds, J. Am. Chem. Soc. 138 (2016) 5825.
[9] H. Huang, J. Asha, J.Y. Kang, Base-controlled Fe(Pc)-catalyzed aerobic oxidation of thiols for the synthesis of S-S and S-P(O) bonds, Org. Biomol. Chem. 16 (2018) 4236.
[10] B. Kaboudin, Y. Abedi, J.Y. Kato, T. Yokomatsu, Copper(I) iodide catalyzed synthesis of thiophosphates by coupling of *H*-phosphonates with benzenethiols, Synthesis 45 (2013) 2323.
[11] J.W. Xue, M. Zeng, S.C. Zhang, Z.Q. Chen, G.C. Yin, Lewis acid promoted aerobic oxidative coupling of thiols with phosphonates by simple nickel(II) catalyst: substrate scope and mechanistic studies, J. Org. Chem. 84 (2019) 4179.
[12] E. Margui, C. Fontas, A. Buend, M. Hidalgo, I. Queralt, Determination of metal residues in active pharmaceutical ingredientsaccording to European current legislation by using X-ray fluorescence spectrometry, J. Anal. At. Spectrom. 24 (2009) 1253.
[13] S. Song, Y.Q. Zhang, A. Yeerlan, B.C. Zhu, J.Z. Liu, N. Jiao, $Cs_2CO_3$-catalyzed aerobic oxidative cross-dehydrogenative coupling of thiols with phosphonates and arenes, Angew. Chem. Int. Ed. 129 (2017) 2527.
[14] J.C. Wang, X. Huang, Z.Q. Ni, Y.J. Pan, J. Wu, Peroxide promoted metal-free thiolation of phosphites by thiophenols/disulfides, Tetrahedron 71 (2015) 7853.
[15] X.J. Bi, J.C. Li, F.H. Meng, H.M. Wang, J.H. Xiao, DCDMH-promoted synthesis of thiophosphates by coupling of *H*-phosphonates with thiols, Tetrahedron 72 (2016) 706.
[16] W. He, X. Hou, X.J. Li, L. Song, Q. Yu, Z.W. Wang, Synthesis of P(O)-S organophosphorus compounds by dehydrogenative coupling reaction of P(O)H compounds with aryl thiols in the presence of base and air, Tetrahedron 73 (2017) 3133.
[17] H. Zhang, Z. Zhan, Y. Lin, Y.S. Shi, G.B. Li, Q.T. Wang, Y. Deng, L. Hai, Y. Wu, Visible light photoredox catalyzed thiophosphate synthesis using methylene blue as a promoter, Org. Chem. Front. 5 (2018) 1416.
[18] Y.C. Liu, C.F. Lee, *N*-Chlorosuccinimide-promoted synthesis of thiophosphates from thiols and phosphonates under mild conditions, Green Chem. 16 (2014) 357.
[19] S. Mohle, M. Zirbes, E. Rodrigo, T. Gieshoff, A. Wiebe, S.R. Waldvoge, Modern electrochemical aspects for the synthesis of value-added organic products, Angew. Chem. Int. Ed. 57 (2018) 6018.
[20] M. Ameri, A. Asghari, A. Amoozadeh, M. Bakherad, A new approach for one-pot, green synthesis of new polycyclic indoles in aqueous solution, Chin. Chem. Lett. 28 (2017) 1031.
[21] A.J.J. Lennox, S.L. Goes, M.P. Webster, H.F. Koolman, S.W. Djuric, S.S. Stahl, Electrochemical aminoxyl-mediated alpha-cyanation of secondary piperidines for pharmaceutical building block diversification, J. Am. Chem. Soc. 140 (2018) 11227.
[22] O.M. Mulina, N.V. Zhironkina, S.A. Paveliev, D.V. Demchuk, A.O. Terent'ev, Electrochemically induced synthesis of sulfonylated *N*-unsubstituted enamines from vinyl azides and sulfonyl hydrazides, Org. Lett. 22 (2020) 1818.
[23] N. Amri, T. Wirth, Accelerating electrochemical synthesis through automated flow: efficient synthesis of chalcogenophosphites, Synlett 31 (2020) 1894.
[24] L.L. Deng, Y. Wang, H.B. Mei, Y. Pan, J.L. Han, Electrochemical dehydrogenative phosphorylation of alcohols for the synthesis of organophosphinates, J. Org. Chem. 84 (2019) 949.
[25] S.M. Guo, S. Li, W.J. Yan, Z.B. Liang, Z.J. Fu, H. Cai, Environmentally sustainable production and application of acyl phosphates, Green Chem. 22 (2020) 7343.

[26] E.O. Yurko, T.V. Gryaznova, K.V. Kholin, V.V. Khrizanforova, Y.H. Budnikova, External oxidant-free cross-coupling: electrochemically induced aromatic C–H phosphonation of azoles with dialkyl-*H*-phosphonates under silver catalysis, Dalton Trans. 47 (2018) 190.
[27] A. Ollivier, S. Sengmany, M. Rey, T. Martens, E. Léonel, Direct phosphonylation of *N*-carbamate-tetrahydroisoquinoline by convergent paired electrolysis, Synlett 31 (2020) 1191.
[28] T.V. Grayaznova, Y.B. Dudkina, D.R. Islamo, O.N. Kataeva, O.G. Sinyashin, D.A. Vicic, Y.H. Budnikova, Pyridine-directed palladium-catalyzed electrochemical phosphonation of C($sp^2$)–H bond, J. Organomet. Chem. 785 (2015) 68.
[29] S. Torii, H. Tanaka, N. Say, Electrosynthesis of heteroatom-heteroatom bonds. 4. direct cross-coupling of dialkyl (or diaryl) phosphites with disulfides by a sodium bromide promoted electrolytic procedure, J. Org. Chem. 44 (1979) 2938.
[30] Y.J. Li, Q. Yang, L.Q. Yang, N. Lei, K. Zheng, A scalable electrochemical dehydrogenative cross-coupling of P(O)H compounds with RSH/ROH, Chem. Commun. 55 (2019) 4981.
[31] C.Y. Li, Y.C. Liu, Y.X. Li, D.M. Reddy, C.F. Lee, Electrochemical dehydrogenative phosphorylation of thiols, Org. Lett. 21 (2019) 7833.
[32] Y. Chen, M. Li, Z. Gong, Z. Shen, Trichloroisocyanuric acid-promoted thiolation of phosphites by thiols, Phosphorus Sulfur Silicon Relat. Elem. 196 (2020) 19.
[33] C. Chen, P.F. Niu, Z.L. Shen, M.C. Li, Electrochemical sulfenylation of indoles with disulfides mediated by potassium iodide, J. Electrochem. Soc. 165 (2018) G67.
[34] X. Liu, P.F. Niu, J.L. Jin, Z.L. Shen, M.C. Li, Electrochemical access to aryl sulfides from aryl thiols and electronrich arenes with the potassium iodide as a mediator, Electrochim. Acta 331 (2020) 135371.
[35] J.L. Jin, L.M. Zhao, C. Zhang, X. Liu, W.X. Yin, Z.L. Shen, M.C. Li, Electrochemical sulfenylation of 4-hydroxycoumarins with aryl thiols catalyzed by potassium iodide, J. Electrochem. Soc. 168 (2021) 025504.
[36] E.I. Rogers, D.S. Silvester, L. Aldous, C. Hardacre, R.G. Compton, Electrooxidation of the iodides [$C_4$mim]I, LiI, NaI, KI, RbI, and CsI in the room temperature ionic liquid [$C_4$mim][$NTf_2$], J. Phys. Chem. C. 112 (2008) 6551.
[37] V.A. Macagno, M.C. Giordano, Kinetics and mechanisms of electrochemical reactions on platinum with solutions of iodine-sodium iodide in acetonitrile, Electrochim. Acta 14 (1969) 335.
[38] M.R. Scheide, C.R. Nicoleti, G.M. Martins, A.L. Braga, Electrohalogenation of organic compounds, Org. Biomol. Chem. 19 (2021) 2578.
[39] F. Lian, K. Xu, C. Zeng, Indirect electrosynthesis with halogen ions as mediators, Chem. Rec 21 (2021) 1.
[40] K. Liu, C.L. Song, A.W. Lei, Recent advances in iodine mediated electrochemical oxidative cross-coupling, Org. Biomol. Chem. 16 (2018) 2375.
[41] T.J. He, Z.R. Ye, Z.F. Ke, J.M. Huang, Stereoselective synthesis of sulfur-containing $\beta$-enaminonitrile derivatives through electrochemical $Csp^3$–H bond oxidative functionalization of acetonitrile, Nat. Commun. 10 (2019) 833.
[42] Z.Y. Mo, T.R. Swaroop, W. Tong, Y.Z. Zhang, H.T. Tang, Y.M. Pan, H.B. Sun, Z.F. Chen, Electrochemical sulfonylation of thiols with sulfonyl hydrazides: a metal- and oxidant-free protocol for the synthesis of thiosulfonates, Green Chem. 20 (2018) 4428.
[43] R.M.C. Silva, G.A. Camara, M.J. Giz, Electro-oxidation of ethanol on ptrh surfaces partially covered by Sn, Electrochim. Acta 308 (2019) 167.
[44] W. Marynowki, T. Klucznik, K. Baranowska, A. Dołęga, W. Wojnowski, Tri(mesityloxy)silanethiol–the first structurally characterized organoxysilanethiol, Z. Anorg. Allg. Chem. 636 (2010) 685.
[45] Y.M. Zhu, X.Y. Luo, H.Z. Zhi, Y.H. Liao, L.D. Xing, M.Q. Xu, X. Liu, K. Xu, W.S. Li, Diethyl(thiophen-2-ylmethyl)phosphonate a novel multifunctional electrolyte additive for high voltage batteries, J. Mater. Chem. A 6 (2018) 10990.
[46] J.F.L. Filho, E.S. Penido, P.P. Castro, C.A. Silva, L.C.A. Melo, Co-pyrolysis of poultry litter and phosphate and magnesium generates alternative slow-release fertilizer suitable for tropical soils, ACS Sustain. Chem. Eng. 5 (2017) 9043.
[47] N. Davletshina, A. Khabibullina, J. Ushakova, R. Davletshina, D. Islamov, K. Usachev, R. Cherkasov, FTIR spectroscopic analyses of the pentyl {[benzyl(dibutyl)ammonio]methyl}phosphonate copper(II) complex, J. Organomet. Chem. 916 (2020) 121267.
[48] X. Chen, Z. Xiao, H. Chu, B. Wang, A.Y. Peng, Reinvestigation of the iodine–mediated phosphoramidation reaction of amines and $P(OR)_3$ and its synthetic applications, Org. Biomol. Chem. 16 (2018) 6783.
[49] I. Matsuzaki, T. Nakajima, H.A. Liebhafsky, The mechanism of the oscillatory decomposition of hydrogen peroxidebythe $I_2$-$IO_3^-$ couple, Chem. Lett. 3 (1974) 1463.
[50] J. Dhineshkumar, K.R. Prabhu, Cross-hetero-dehydrogenative coupling reaction of phosphites: a catalytic metal free phosphorylation of amines and alcohols, Org. Lett. 15 (2013) 6062.
[51] S.L. Yi, M.C. Li, W.M. Mo, X.Q. Hu, B.X. Hu, N. Sun, L.Q. Jin, Z.L. Shen, Metal-free, iodine-catalyzed regioselective sulfenylation of indoles with thiols, Tetrahedron Lett. 57 (2016) 1912.
[52] P.F. Huang, P. Wang, S. Tang, S. Tang, Z.J. Fu, A.W. Lei, Electro-oxidative S-H/S-H cross-coupling with hydrogen evolution: facile access to unsymmetrical disulfides, Angew. Chem. Int. Ed. 57 (2018) 8115.
[53] K.P. Dockery, W.G. Bentrude, Free radical chain reactions of [1.1.1]propellane with three-coordinate phosphorus molecules. Evidence for the high reactivity of the bicyclo[1.1.1]pent-1-yl radical, J. Am. Chem. Soc. 119 (1997) 1388.
[54] C.K. Li, Z.H. Tao, X.G. Bao, S.F. Zhou, J.P. Zou, Copper-catalyzed oxidative $sp^3$-carbon radical cross-coupling with trialkylphosphites leading to $\alpha$-phosphonyl 1,3-dicarbonyl compounds, J. Org. Chem. 84 (2019) 2351.
[55] Y. Deng, S.Q. You, M.Y. Ruan, Y. Wang, Z.X. Chen, G.C. Yang, M. Gao, Electrochemical regioselective phosphorylation of nitrogen-containing heterocycles and related derivatives, Adv. Synth. Catal. 363 (2021) 464.